

Ground State and Magnetization Process of the Mixture of Bond-Alternating and Uniform $S = 1/2$ Antiferromagnetic Heisenberg Chains

Kazuo HIDA *

Department of Physics, Faculty of Science,
Saitama University, Saitama 338-8570

(Received February 7, 2020)

The mixture of bond-alternating and uniform $S = 1/2$ antiferromagnetic Heisenberg chains is investigated by the density matrix renormalization group method. The ground state magnetization curve is calculated and the exchange parameters are determined by fitting to the experimentally measured magnetization curve of $\text{CuCl}_{2x}\text{Br}_{2(1-x)}(\gamma\text{-pic})_2$. The low field behavior of the magnetization curve and low temperature behavior of the magnetic susceptibility are found to be sensitive to whether the bond-alternation pattern (parity) is fixed all over the sample or randomly distributed. The both quantities are compatible with the numerical results for the random parity model.

KEYWORDS: $\text{CuCl}_{2x}\text{Br}_{2(1-x)}(\gamma\text{-pic})_2$, random Heisenberg chain, density matrix renormalization group, magnetization process, random singlet phase, quantum Griffiths phase

1. Introduction

In recent studies of quantum many body problem, the ground state properties of the random quantum systems have been attracting a renewed interest. Among them, the effect of randomness in one-dimensional quantum spin systems has been extensively studied theoretically and experimentally.¹⁻¹³⁾

The real space renormalization group (RSRG) analysis of the $S = 1/2$ random bond antiferromagnetic Heisenberg chain¹⁻³⁾ has shown that the ground state of the $S = 1/2$ uniform antiferromagnetic Heisenberg chain is unstable against the bond randomness of infinitesimal strength and the random singlet phase is realized in which the spins form singlet pairs randomly with distant partners.³⁾ In this phase, the spin-spin correlation decays by the power law with exponent -2 and log-averaged energy gap scales as $\langle \ln \Delta \rangle \simeq -\alpha \sqrt{N} + \text{const.}$, where N is the system size and α is a constant. This has been confirmed numerically⁴⁾ by means of the density matrix renormalization group (DMRG) method.¹⁴⁾

On the other hand, the effect of randomness on the spin gap state of one-dimensional quantum spin systems has been extensively studied⁵⁻¹¹⁾ related with the doping effect in bond-alternating chains^{8,9)} and spin ladders.¹⁰⁾ Hyman and coworkers^{5,6)} have applied the RSRG method to the spin-1/2 random dimerized antiferromagnetic Heisenberg chain and have shown that the dimerization is a relevant perturbation to the random singlet phase^{5,6)}. This implies that the ground state of the spin-1/2 dimerized antiferromagnetic Heisenberg chain is stable against infinitesimal randomness. They also argued that the ground state of this model is the random dimer phase which belongs to the quantum Griffiths phase in which the spin-spin correlation length is finite and log-averaged energy gap scales as $\langle \ln \Delta \rangle \sim -z \ln N + \text{const.}$ with finite dynamical exponent z . This is also verified by the DMRG calculation by the present author.⁷⁾

Motivated by the quite distinct nature of the uniform

chain and bond-alternating chain against randomness, Ajiro and coworkers experimentally investigated the magnetic properties of the compound $\text{CuCl}_{2x}\text{Br}_{2(1-x)}(\gamma\text{-pic})_2$ ^{12,13)} which is the mixed compound of $S = 1/2$ uniform and bond-alternating antiferromagnetic Heisenberg chains. The $x = 1$ compound $\text{CuCl}_2(\gamma\text{-pic})_2$ is an $S = 1/2$ bond-alternating antiferromagnetic Heisenberg chain¹⁵⁾ and the $x = 0$ compound $\text{CuBr}_2(\gamma\text{-pic})_2$ is an $S = 1/2$ uniform antiferromagnetic Heisenberg chain.¹²⁾ In order to understand the low temperature magnetic properties of these compounds, we theoretically investigate the ground state and low energy properties of the mixture of bond-alternating and uniform $S = 1/2$ antiferromagnetic Heisenberg chains using DMRG method in the present work.

This paper is organized as follows. In the next section, the theoretical model which describes the mixed compound $\text{CuCl}_{2x}\text{Br}_{2(1-x)}(\gamma\text{-pic})_2$ is presented. In section 3, the magnetization curve is calculated and the exchange parameters are determined from overall behavior of the magnetization curve. The numerical results of the low energy magnetic excitation spectrum is presented in section 4. Based on the finite size scaling analysis of the log-averaged energy gap, the low temperature singularity of the magnetic susceptibility is predicted and the explanation of the experimentally observed temperature dependence of susceptibility data is given. The last section is devoted to summary and discussion.

2. Theoretical Model of $\text{CuCl}_{2x}\text{Br}_{2(1-x)}(\gamma\text{-pic})_2$

In the compound $\text{CuCl}_{2x}\text{Br}_{2(1-x)}(\gamma\text{-pic})_2$, the Cu-Cu bond is bridged by Cl and/or Br ions, so that there exist $\text{Cu} < \text{Cl} > \text{Cu}$, $\text{Cu} < \text{Br} > \text{Cu}$ and $\text{Cu} < \text{Br} > \text{Cu}$ bonds in this compound. In the pure compound $\text{CuCl}_2(\gamma\text{-pic})_2$, two kinds of $\text{Cu} < \text{Cl} > \text{Cu}$ bonds alternate along the chain, although this material appears to be a uniform chain from chemical formula. This bond alternation is induced by the freezing transition of rotational motion of methyl-group at 50K.¹⁵⁾ For finite Br-concentration

($0 < x < 1$), this compound can be regarded as an assembly of the finite length clusters connected only by the Cu $\langle \text{Cl} \rangle$ Cu bonds (hereafter called 'bond-alternating cluster'; abbreviated as BAC) with Cu $\langle \text{Br} \rangle$ Cu and/or Cu $\langle \text{Cl} \rangle$ Cu bonds in between. However, it is not obvious whether the rotational order of methyl-group remains long ranged even in the mixed compound. If this order is long ranged, the bond alternation pattern is common among different BAC's even though they are separated by Cu $\langle \text{Br} \rangle$ Cu or Cu $\langle \text{Cl} \rangle$ Cu bonds. In what follows, this case is called *fixed parity* case. On the other hand, if the rotational order of methyl-group is also cut into short range order by Br-substitution on Cl sites, the bond alternation patterns of the Cu $\langle \text{Cl} \rangle$ Cu bonds are uncorrelated among different BAC's once they are separated by Cu $\langle \text{Cl} \rangle$ Cu or Cu $\langle \text{Br} \rangle$ Cu bonds. This case is called *random parity* case. For the moment, there is no experimental evidence which case is realized in $\text{CuCl}_{2x}\text{Br}_{2(1-x)}(\gamma\text{-pic})_2$. In the following, we therefore investigate both cases theoretically.

The strength of these bonds are denoted by J (strong Cu $\langle \text{Cl} \rangle$ Cu bond), αJ (weak Cu $\langle \text{Cl} \rangle$ Cu bond), J' (Cu $\langle \text{Br} \rangle$ Cu bond) and J'' (Cu $\langle \text{Br} \rangle$ Cu bond), respectively in the following Hamiltonian which describes the mixed chain.

$$H = \sum_{i=1}^N 2J_i \mathbf{S}_i \mathbf{S}_{i+1}, \quad (1)$$

$$J_i = \begin{cases} J & \text{for } i + i_p = \text{even} \\ \alpha J & \text{for } i + i_p = \text{odd} \\ J' & \\ J'' & \end{cases} \quad p = x^2, \quad p = 2x(1-x), \quad p = (1-x)^2, \quad (2)$$

where p is the probability of realization of each type of bonds. We define the integer 'parity' i_p for each BAC. Corresponding to the fixed and random parity cases explained above, the parity i_p takes the following values in each cases.

- (1) Random parity case : i_p takes the values 0 or 1 randomly in different BAC's.
- (2) Fixed parity case : $i_p = 0$ for all BAC's.

The possible local bond configurations realized in each case can be visually explained using Fig. 1. The uppermost configuration R shows the regular bond-alternating chain corresponding to $\text{CuCl}_2(\gamma\text{-pic})_2$. The local configurations of type-A and B can occur in the mixed chain $\text{CuCl}_{2x}\text{Br}_{2(1-x)}(\gamma\text{-pic})_2$. The two BAC's in type-A configuration are in phase with regular chain R. On the other hand, in type-B configuration, the left BAC in the solid rectangle is in phase with R while the right BAC in the dotted rectangle is out of phase from R. The local configurations of type-A and B (with its mirror inversion) occur with the same weight in the random parity case but only type-A configuration occurs in the fixed parity case.

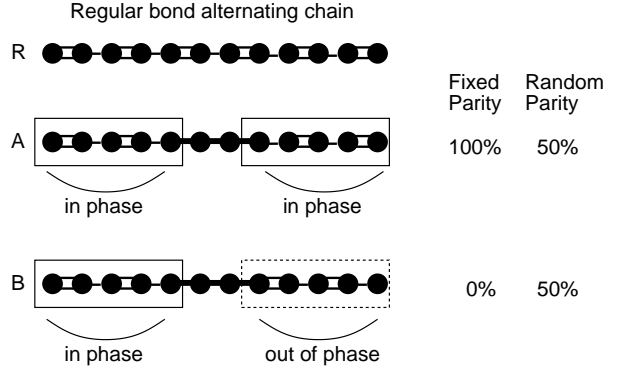


Fig. 1. Schematic view of the local bond configuration. The thick lines denote the Cu $\langle \text{Br} \rangle$ Cu or Cu $\langle \text{Cl} \rangle$ Cu bonds and the thin single and double lines, the alternating Cu $\langle \text{Cl} \rangle$ Cu bonds. The uppermost configuration R corresponds to the regular bond-alternating chain ($\text{CuCl}_2(\gamma\text{-pic})_2$). Two possible local bond configurations in the mixed chain $\text{CuCl}_{2x}\text{Br}_{2(1-x)}(\gamma\text{-pic})_2$ are shown as A and B. The clusters in the rectangles are bond-alternating clusters (BAC's). In the random parity case, the type-A and type-B configurations occur with the same weight. In the fixed parity case, only type-A configuration occurs.

3. Magnetization Process

From the measurement for the pure systems ($x = 0, 1$), the coupling constants J, α and J'' are determined as,^{12,13}

$$J = 13.2\text{K}, \quad J'' = 20.3\text{K}, \quad \alpha = 0.6. \quad (3)$$

Using these parameters, we have calculated the magnetization curve of the mixed chain using DMRG method for various choices of J' and determined $J'/J = 1.3$ so as to reproduce the overall magnetization curve of $\text{CuCl}_{2x}\text{Br}_{2(1-x)}(\gamma\text{-pic})_2$. The chain length N is fixed to 100 and the average is taken over 100 samples. The maximum number of the states kept in each subsystem in the course of DMRG calculation is 300. It should be noted that the overall magnetization curve does not depend whether the parity is fixed or random, except for the low field part where the magnetization curve is more convex in the random parity model as shown in Fig. 2. The low field part of the magnetization curve reported in refs. 12 and 13 seems to be consistent with the random parity model. However, due to the finite temperature effect in the experimental data and finite size effect in the numerical calculation, the direct quantitative comparison is difficult. Actually, the most significant difference between the two models is the low field singularity of the magnetization determined by the low energy singularity of the magnetic excitation spectrum. At finite temperatures, however, this singularity is rounded to yield finite magnetic susceptibility which diverges or vanishes as the temperature is lowered. Therefore, for the quantitative comparison with experiment, we concentrate on the low temperature singularity of the susceptibility which can be deduced from the finite size scaling analysis of the low energy magnetic excitation spectrum in the next section.

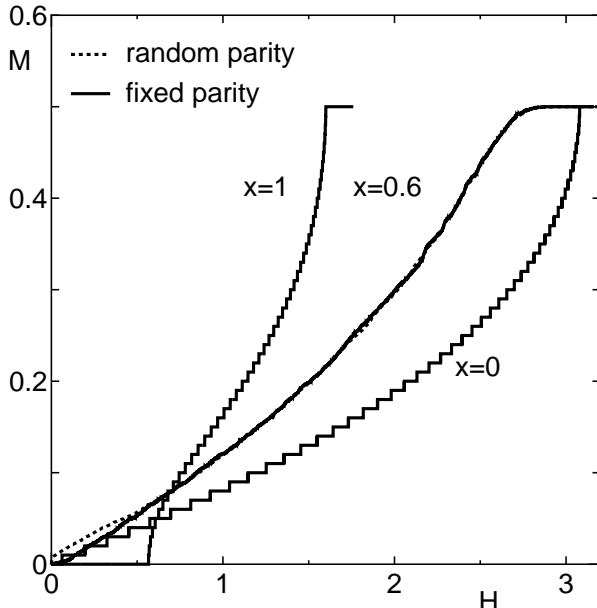


Fig. 2. Magnetization curves of the fixed parity model (solid line) and random parity model (dotted line) with $x = 0.6$. The step-wise lines are the magnetization processes of pure systems ($x = 0$ and $x = 1$). For $x = 0.6$, the error bars are comparable with the width of the lines.

4. Low energy magnetic excitation spectrum

4.1 Fixed parity case

The lowest excitation gaps with total magnetization $S_z^{\text{tot}} = 1$ for each sample is calculated using the infinite size DMRG method⁴⁾ for $10 \leq N \leq 80$ ($x \leq 0.5$) and for $10 \leq N \leq 160$ ($x \geq 0.6$). The average is taken over 200 samples. The number of the states kept in each subsystem during the course of the DMRG calculation is 60. The accuracy is confirmed by checking the coincidence of the energy gap with $(S_{\text{tot}}, S_{\text{tot}}^z) = (1, 0)$ and that with $(S_{\text{tot}}, S_{\text{tot}}^z) = (1, 1)$ taking into account the $SU(2)$ symmetry of the present system.

The log-averaged energy gap $\langle \ln \Delta \rangle$ is plotted against $\ln N$ in Fig. 3 which show a fairly good linear behavior

$$\langle \ln \Delta \rangle = \ln \Delta_0 - z \ln N, \quad (4)$$

for large N and $x \geq 0.4$. For $x \leq 0.3$, the data are not well fitted by (4). Presumably, in this regime, the concentration of the alternating bond x^2 is too small and true asymptotic behavior is not observable for the present system sizes. This result implies that the ground state of this model is the quantum Griffiths phase characterized by the finite dynamical exponent z at least for $x \geq 0.4$. In the quantum Griffiths phase, the low temperature susceptibility $\chi(T)$ and low field magnetization at zero temperature $M(H)$ should behave as $\chi(T) \sim T^{1/z-1}$ and $M(H) \sim H^{1/z}$.^{5,6)}

Physically, this result is reasonable. In this model, the dimerization pattern is fixed over the whole system. As pointed out by Hyman and coworkers,⁵⁾ the dimerization is a relevant perturbation to the random singlet phase and drives the system into the random dimer phase which belongs to the quantum Griffiths phase.

In the experiment, it is found that the low temperature susceptibility of $\text{CuCl}_{2x}\text{Br}_{2(1-x)}(\gamma\text{-pic})_2$ shows a divergent behavior as $\chi \sim T^{\beta-1}$ with an exponent $\beta \sim 0.67$.^{12,13,16)} The value of β slightly depends on the concentration x . At first sight, the above result appears to be consistent with the prediction of the fixed parity model, if we identify $z = 1/\beta$ as proposed in ref. 12. Based on this idea, we determine the exponent z by fitting $\langle \ln \Delta \rangle$ in Fig. 3 by Eq. (4). The result is shown in Fig. 4 in terms of $\beta = 1/z$. Although the value of β for small x is difficult to determine from the numerical data, we may expect it would roughly behave as shown by the dotted line considering that $\beta = 1$ for $x = 0$ (Luttinger liquid). The exponent β is, however, always larger than or around unity as shown in Fig. 4 within the regime $x \geq 0.4$. Therefore the fixed parity model does not explain the experimentally observed exponent $\beta \sim 0.67$. Actually, if we look into the experimental data closely, the exponent β turns out to decrease with x , although the temperature of the experiment is not low enough to exclude the contribution of higher energy excitations. On the contrary, in the fixed parity model, β increases rapidly with x for $x \gtrsim 0.4$ as shown in Fig. 4. The physical reason of the sharp increase of β is obvious. In the limit $x \rightarrow 1$, the system is gapped, so that z should tend to zero.

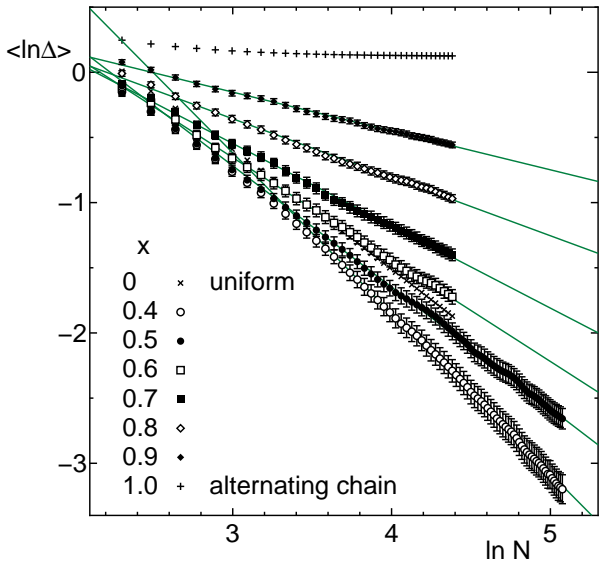


Fig. 3. System size dependence of $\langle \ln \Delta \rangle$ in the fixed parity case. The gap is measured in units of J .

4.2 Random parity case

In this case also, the lowest excitation gaps with total magnetization $S_z^{\text{tot}} = 1$ for each sample is calculated using the DMRG method for $N \leq 80$ in the same way as in the preceding subsection. The maximum number m of the state kept in the course of DMRG calculation is $m = 200$.

The log-averaged magnetic energy gap $\langle \ln \Delta \rangle$ is plotted against \sqrt{N} in Fig. 5 which show a fairly good linear behavior

$$\langle \ln \Delta \rangle = \ln \Delta_0 - \alpha \sqrt{N}. \quad (5)$$

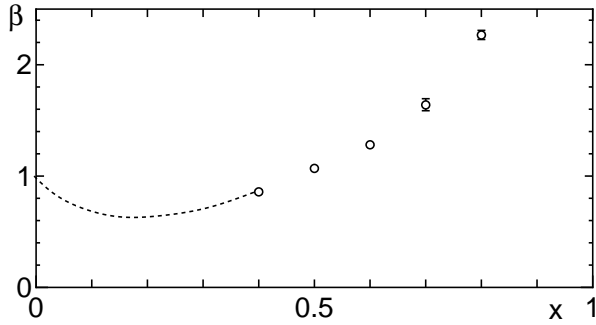


Fig. 4. The exponent β plotted against x in the fixed parity case.

This implies that the ground state is the random singlet state in which the low temperature susceptibility $\chi(T)$ and low field magnetization at zero temperature $M(H)$ should behave as $\chi(T) \sim 1/(T(\ln T)^2)$ and $M(H) \sim (\ln(1/H))^{-2}$.³⁾ In this case, the dimerization pattern is not long ranged. Therefore the translational symmetry is preserved on average and the random singlet phase remains stable.

However, it should be noted that this asymptotic form for χ is only valid in the true low temperature limit. At finite temperatures, we may define the temperature dependent effective value of z even in the random parity case in the following way.

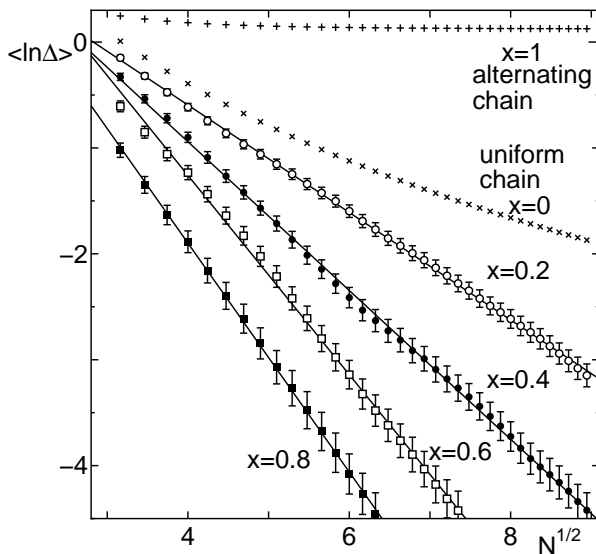


Fig. 5. System size dependence of $\langle \ln \Delta \rangle$ in the random parity case. The gap is measured in units of J .

Let us define the size dependent effective value of z by

$$z_{\text{eff}} \equiv -\frac{d \langle \ln \Delta \rangle}{d \ln N}, \quad (6)$$

based on the formula (4). This size dependent exponent can be interpreted as the energy dependent effective exponent because the typical energy scale of the cluster is related with the cluster size N by the relation (5). Thus we find that z_{eff} is given by

$$z_{\text{eff}} = \frac{\alpha}{2} \sqrt{N} = \frac{1}{2} \langle \ln \left(\frac{\Delta_0}{\Delta} \right) \rangle. \quad (7)$$

Therefore, in the temperature range around T , we can define the temperature dependent effective value of z by

$$z_{\text{eff}}(T) = \frac{1}{2} \ln \left(\frac{\Delta_0}{k_B T} \right) \quad (8)$$

by setting $\langle \ln \Delta \rangle = \ln(k_B T)$ in (7).

From the fit to (5) we have determined the value of Δ_0 . Around the temperature range where the measurement is made ($T \gtrsim 2\text{K}$), the values of the effective exponent $\beta_{\text{eff}}(T) \equiv 1/z_{\text{eff}}(T)$ are plotted against T in Fig. 6 for various values of x . They are also plotted against x for $T = 2\text{K}$ and 4K in Fig. 7. It is clearly seen that β_{eff} ranges from 0.4 to 0.7 for $0.8 \geq x \geq 0.2$. This explains why the measured susceptibility exponent is around these values. Especially, at the fixed temperature, the exponent β decreases with x in accordance with the experimental tendency.

Physically, the x -dependence of β_{eff} is understood as follows. The quantity Δ_0 is essentially the bare energy scale of the system. In the spirit of RSRG method for random quantum spin chains,¹⁻³⁾ it is of the order of the largest exchange coupling $2J'' \sim 40.6\text{K}$ which is decimated in the first step renormalization. Therefore we may roughly estimate as $\beta_{\text{eff}} \sim 2/\ln(2J''/k_B T) \sim 0.66$ at $T = 2\text{K}$ and this value is insensitive to x . However, as x approaches zero, the ground state should tend to the Luttinger liquid characterized by $z = \beta = 1$. Therefore β_{eff} increases to approach this value with the decrease of x . Actually, for small x , there exist many large uniform clusters coupled with the strongest bond J'' so that the first step renormalization cannot start with the single bond. Therefore, the effective value of Δ_0 is reduced from J'' and β_{eff} is enhanced.

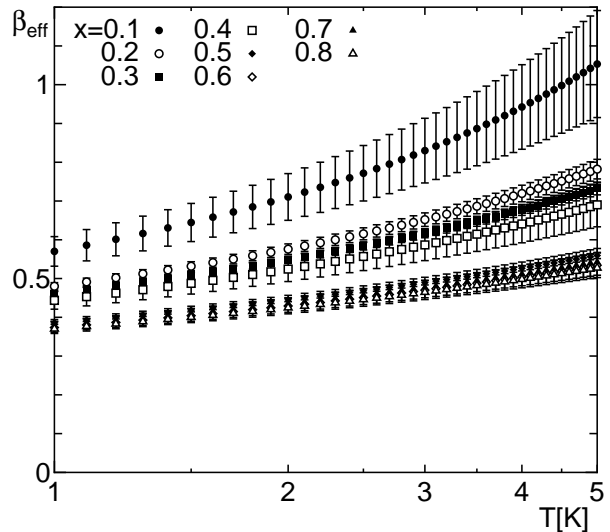


Fig. 6. The effective exponent β_{eff} plotted against temperature $T\text{K}$.

5. Summary

The magnetization process of the mixture of uniform and alternating-bond $S = 1/2$ antiferromagnetic Heisenberg chain is calculated using the DMRG method in the ground state. The magnetization processes of random

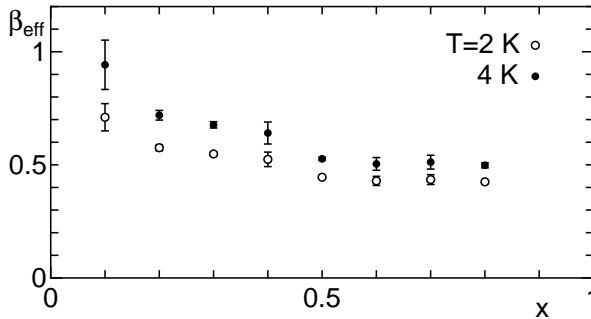


Fig. 7. The effective exponent β_{eff} plotted against Cl concentration x .

and fixed parity cases are similar to each other except for the low field singularity which reflects the low energy spectrum. Comparing with the experimental magnetization curve for $\text{CuCl}_{2x}\text{Br}_{2(1-x)}(\gamma\text{-pic})_2$ the exchange parameters are determined. The low field magnetization curve of $\text{CuCl}_{2x}\text{Br}_{2(1-x)}(\gamma\text{-pic})_2$ looks similar to that of the random parity case although the direct comparison is difficult due to the finite temperature effect in experiment and finite size effect in numerical calculation.

For the quantitative analysis of the low field limit, the low energy energy spectrum obtained by the DMRG method is analyzed using the finite size scaling method. The ground state is the random singlet phase for the random parity model and it is the quantum Griffiths phase in the fixed parity model. The low temperature singularity of the experimentally observed susceptibility of $\text{CuCl}_{2x}\text{Br}_{2(1-x)}(\gamma\text{-pic})_2$ is consistent with the theoretical results for the random parity model assuming the temperature dependent effective exponent β_{eff} .

It should be noted that our calculation predicts that the effective value of β decreases with the Cl concentration for $x \lesssim 0.5$. Although this seems to be compatible with the experimental data, more precise measurement of susceptibility at lower temperatures is hoped in the

future including the possibility of direct measurement of the random singlet behavior $\chi(T) \sim 1/(T(\ln T)^2)$.

The author is grateful to Y. Ajiro for valuable discussion and for explaining the details of the analysis of the experimental data. The computation in this work has been done using the facilities of the Supercomputer Center, Institute for Solid State Physics, University of Tokyo and the Information Processing Center, Saitama University. This work is supported by a Grant-in-Aid for Scientific Research from the Ministry of Education, Culture, Sports, Science and Technology, Japan.

- 1) S.-k. Ma, C. Dasgupta and C. K. Hu: *Phys. Rev. Lett.* **43** (1979) 1434.
- 2) C. Dasgupta and S.-k. Ma: *Phys. Rev. B* **22** (1980) 1305.
- 3) D. S. Fisher: *Phys. Rev. B* **50** (1994) 3799.
- 4) K. Hida: *J. Phys. Soc. Jpn.* **65** (1996) 895; errata *ibid.* **3412**.
- 5) R. A. Hyman, K. Yang, R. N. Bhatt and S. M. Girvin: *Phys. Rev. Lett.* **76** (1996) 839.
- 6) R. A. Hyman and K. Yang: *Phys. Rev. Lett.* **78** (1997) 1783.
- 7) K. Hida: *J. Phys. Soc. Jpn.* **66** (1997) 3237.
- 8) K. Uchinokura: *Prog. Theor. Phys. Suppl.* **145** (2002) 296 and references therein.
- 9) Y. Uchiyama, Y. Sasago, I. Tsukada, K. Uchinokura, A. Zheludev, T. Hayashi, N. Miura, and P. Boni: *Phys. Rev. Lett.* **83**, (1999) 632.
- 10) M. Azuma, Y. Fujishiro, M. Takano, M. Nohara and H. Takagi : *Phys. Rev. B* **55**, (1997) R8658.
- 11) H. Fukuyama, T. Tanimoto and M. Saito: *J. Phys. Soc. Jpn.* **65** (1996) 1182. *Rev. B* **64**, 092405 (2001).
- 12) Y. Ajiro, T. Wakisaka, H. Itoh, K. Watanabe, H. Satoh, Y. Inagaki , T. Asano, M. Mito, K. Takeda, H. Mitamura and T. Goto: *Physica B* in press (2003).
- 13) T. Wakisaka: Master Thesis (in Japanese), Kyushu University (2003).
- 14) S. R. White: *Phys. Rev. Lett.* **69** (1992) 2863; *Phys. Rev. B* **48** (1993) 10345.
- 15) H. J. M. de Groot, L. J. de Jongh and R. D. Willett: *J. Appl. Phys.* **53** 8038 (1982).
- 16) Y. Ajiro: private communication. In ref. 12 this value is reported as $\beta = 0.5$ but the experimental data are better fitted by $\beta = 0.67$ as reported in ref. 13.